Time-reversed ultrasonically encoded (TRUE) optical focusing in reflection mode: demonstrations in tissue mimicking phantoms and ex vivo tissue

Puxiang Lai, Xiao Xu, Honglin Liu, Yuta Suzuki, Lihong V. Wang

Puxiang Lai, Xiao Xu, Honglin Liu, Yuta Suzuki, Lihong V. Wang, "Time-reversed ultrasonically encoded (TRUE) optical focusing in reflection mode: demonstrations in tissue mimicking phantoms and ex vivo tissue," Proc. SPIE 8223, Photons Plus Ultrasound: Imaging and Sensing 2012, 82231B (9 February 2012); doi: 10.1117/12.906017

SPIE.

Event: SPIE BiOS, 2012, San Francisco, California, United States

Time-Reversed Ultrasonically Encoded (TRUE) Optical Focusing in Reflection Mode: Demonstrations in Tissue Mimicking Phantoms and *ex vivo* Tissue

Puxiang Lai, Xiao Xu, Honglin Liu, Yuta Suzuki, and Lihong V. Wang

Washington University in St. Louis
Department of Biomedical Engineering, Optical Imaging Laboratory
Campus Box 1097, 1 Brookings Drive, St. Louis, Missouri 63130, USA

ABSTRACT

The problem of how to effectively deliver light dynamically to a small volume inside turbid media has been intensively investigated for imaging and therapeutic purposes. Most recently, a new modality termed Time-Reversed Ultrasonically Encoded (TRUE) optical focusing was proposed by integrating the concepts of ultrasound modulation of diffused light with optical phase conjugation. In this work, the diffused photons that travel through the ultrasound focal region are "tagged" with a frequency shift due to the ultrasound modulation. Part of the tagged light is collected in reflection mode and transmitted to a photorefractive crystal, forming there a stationary hologram through interference with a coherent reference optical beam. The hologram is later read by a conjugated optical beam, generating a phase conjugated wavefront of the tagged light. It is conveyed back to the turbid medium in reflection mode, and eventually converges to the ultrasound focal zone. Optical focusing effects from this system are demonstrated experimentally in tissue-mimicking phantoms and *ex vivo* chicken breast tissue, achieving effective round-trip optical penetration pathlength (extinction coefficient multiplied by round-trip focusing depth) exceeding 160 and 100, respectively. Examples of imaging optical inclusions with this system are also reported.

Keywords: optical focusing, optical imaging, ultrasound modulation, optical phase conjugation, phase conjugation mirror, time reversal, photorefractive crystal, reflection mode, tissue-mimicking phantom, biological tissue, optical fiber bundle

1. INTRODUCTION

Light has been playing a more and more important role in biomedical sensing and disease treatment. Its usage, however, is inherently limited by the multiple scattering of light in tissue, resulting in a compromised spatial resolution at depths beyond one transport mean free path (typically ~ 1 mm in human skin)[1] (Fig. 1a). Therefore, the problem of how to effectively deliver light dynamically to a small volume inside turbid media has been intensively investigated. One

Further author information: Puxiang Lai, plai@wustl.edu, 1-314-935 9587
Lihong V. Wang, lhwang@biomed.wustl.edu, 1-314- 935 6152

Photons Plus Ultrasound: Imaging and Sensing 2012, edited by Alexander A. Oraevsky, Lihong V. Wang,
Proc. of SPIE Vol. 8223, 82231B · © 2012 SPIE · CCC code: 1605-7422/12/$18 · doi: 10.1117/12.906017

representative is wavefront shaping[2, 3]. In this technique, a spatial light modulator is used to adjust the relative phases of an incident beam's wavefront, and a closed-loop feedback method is used to maximize the resultant light intensity at a desired focal point inside or beyond a turbid medium (Fig. 1b). For high quality focusing, however, this approach usually requires a large number of independently controllable segments on the spatial light modulator, causing an extensive amount of computation. Another promising approach is optical phase conjugation[4] that uses a phase conjugation mirror to generate a phase conjugated wavefront copy of the initial diffused light. Due to the reversibility of light propagation, the conjugated wavefront can travel back through the turbid medium, following the opposite direction of the initial light (Fig. 1c). However, since there is no internal source inside the turbid medium, the reversed light can only be focused again outside the turbid medium. This limitation hinders this approach from wide applications. If an ultrasound field is applied to modulate the propagation of diffused light inside the turbid medium, photons traversing the ultrasound focal region will be encoded with an ultrasonic frequency shift (Fig. 1d) through the displacements of scatterers and the variation in the medium's index of refraction[5]. In this case, if the resultant diffused light is collected outside the turbid medium and sent to a phase conjugation mirror (PCM) that is only sensitive to the ultrasonically encoded light, the reversed conjugated light will travel back, although tortuously, to the ultrasound focus inside the turbid medium (Fig. 1e). The ultrasound focus, in this sense, serves as a virtual internal source. The combination of ultrasound encoding with optical phase conjugation brings the invention of time-reversed ultrasonically-encoded (TRUE) optical focusing that was first published in early 2011[6].

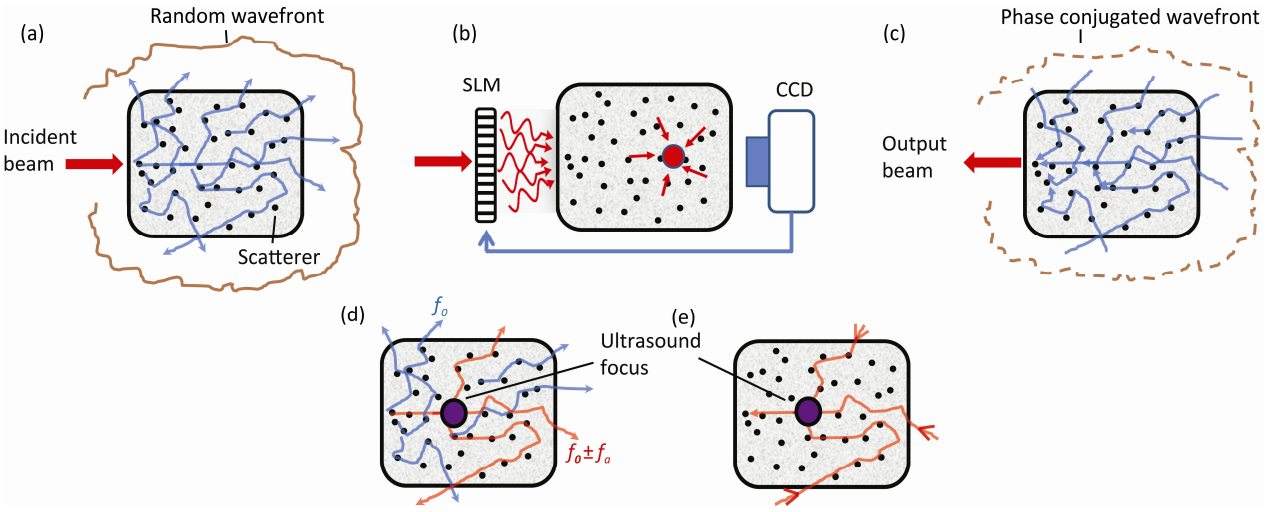

Fig. 1 (a) Photons are multiply scattered within a turbid medium, resulting a random wavefront output. (b) Wavefront shaping method to maximize the resultant light intensity inside or beyond a turbid medium through adjusting the relative phases of an incident light beam's wavefront via a spatial light modulator (SLM). (c) Optical phase conjugation method to generate a phase conjugated wavefront copy of the initial diffused light, which travel back to the turbid medium following the opposite direction to the initial light. (d) Photons (initially with a central frequency f_0) traversing the ultrasound focus are encoded with an ultrasound frequency shift (f_a). (e) When the phase conjugation mirror is set only sensitive to the ultrasonically-encoded photons, the reversed light will travel back and eventually refocus again at the ultrasound focus within the turbid medium.

2. METHODOLOGY AND MATERIALS

The concept of TRUE optical focusing was first implemented in transmission mode[6, 7], where light incidence and collection were on opposite sides of the turbid medium. Such an alignment may pose limitations on applications on medical imaging where transmitting illumination leads to an undesirable increase in operative optical penetration. To make this new technique more practical and convenient, we developed a reflection-mode TRUE optical focusing system[8, 9], in which the optical input and output modules are installed on the same side of the experiment sample. The experimental setup is illustrated in Fig. 2.

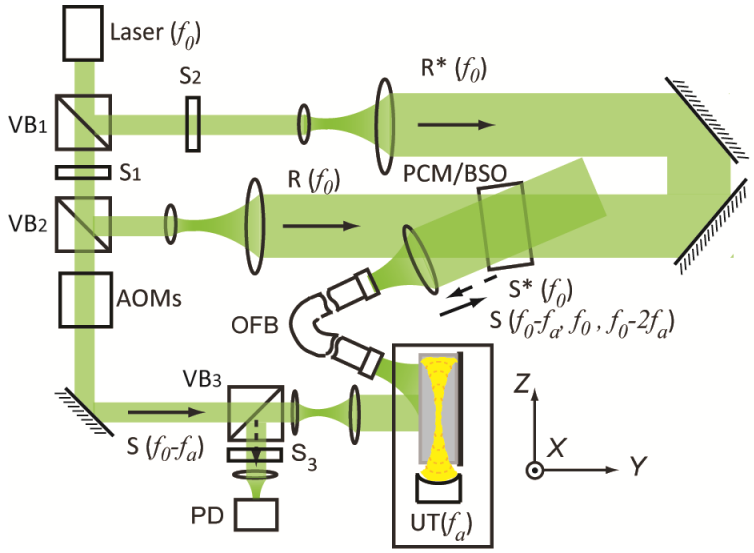

Fig. 2. System apparatus: *XYZ*, system coordinates (*Y* is the optical illumination direction, and *Z* is the ultrasound propagation direction); $VBS_{1\text{-}3}$, variable beam splitters, each composed of a half-wave plate and a polarizing beam splitter; $S_{1\text{-}3}$, shutters; AOMs, two acousto-optic modulators functioning in series; PD, photodiode detector; UT, ultrasound transducer; OFB, optical fiber bundle (light guide); BSO, $Bi_{12}SiO_2$ photorefractive crystal (used as the PCM); f_0, frequency of the laser; f_a, frequency of the ultrasound; $S(f_0 - f_a)$, light incident onto the turbid sample surface; $S(f_0 - f_a, f_0, f_0 - 2f_a)$, reflectively collected diffused light from the sample; $R(f_0)$, the reference beam; $R^*(f_0)$, the conjugate reading beam; $S^*(f_0)$, the time-reversed copy of $S(f_0)$.

As shown, the laser output from a 532 nm laser (Verdi V-10, Coherent) was split into three beams: signal beam (*S*), reference beam (*R*), and reading beam (*R**). Within each system cycle (1 s), the reading beam was blocked during the first 190 ms by S_2. The signal beam was expanded and illuminated the diffuse sample, inside which photons are multiply scattered and modulated by the ultrasound. The resultant scattered light, including both modulated and unmodulated portions, was collected in reflection mode using a large aperture (0.5 inch diameter), high *NA* (0.55) optical fiber bundle (OFB in Fig. 2), and was transmitted onto a photorefractive BSO crystal (PRC) that was used as a PCM. The signal beam interfered with the reference beam within the crystal, but the crystal was set to be only sensitive to the photons having the same frequency at f_0, i.e. ultrasonically-encoded photons. In the subsequent reading stage from 190 ms, the signal beam and reference beam were both blocked, and the reading beam was now allowed to propagate along the opposite direction to the reference beam, generating a phase conjugated wavefront of $S(f_0)$, $S^*(f_0)$. This reversed signal travelled back into the turbid medium, and eventually converged to the ultrasound focus. A photodiode (PD in Fig. 2) was used to record the signal back-scattered again from the ultrasound focus. In the study, the ultrasound field for modulation was 200 ms long

temporally, and 0.87 mm wide laterally at its focal waist. It had a central frequency of 3.5 MHz, and a peak-to-peak focal pressure of 1-1.33 MPa. To assure best acoustic impedance match along the acoustic path, the scattering medium, including both tissue-mimicking phantom and tissue, was sandwiched between two transparent gelatin gel layers in the *Y* direction as shown in Fig. 3. Note that to embed the optical inhomogeneities at the central Y plane, the scattering medium was actually prepared as two layers in the Y direction before and after the inclusions. During the experiment, the sample was partially submerged in water in the *Z* direction, and the front surface of the turbid layer was denoted as $Y = 0$.

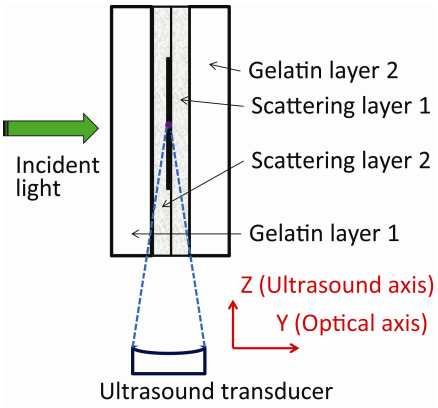

Fig. 3 Illustration of turbid sample preparation and its position with respect to the incident light and the ultrasound.

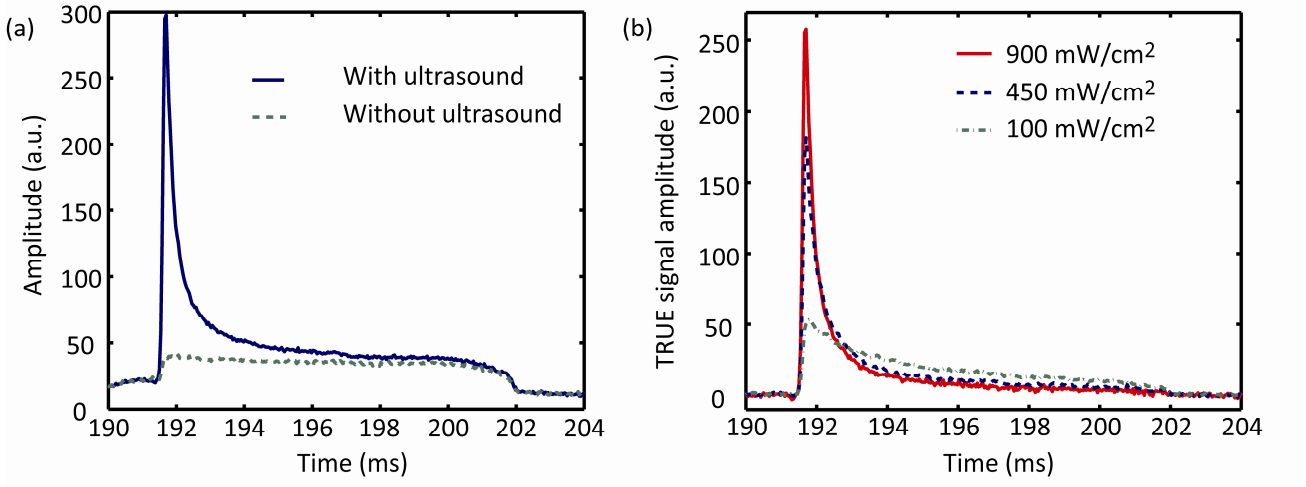

Fig. 4 (a) Examples of optical signal detected at the photodiode with (blue, solid curve) and without (green, dashed curve) ultrasound modulation. (b) Subtracted TRUE signals with different reading beam intensities (red, solid curve- 900 mW/cm^2; blue, dashed curve- 450 mW/cm^2; green, dash-dots curve- 100 mW/cm^2).

Fig. 4(a) shows an example of optical signal detected at the photodiode without ultrasound modulation (green, dashed curve) through a scattering medium with aforementioned parameters. Since no time reversed signal is generated due to the lack of ultrasound modulation, we see a relatively flat background within the duration when S_2 is opened and closed. This background comes from the randomly scattered reading beam. With ultrasound modulation, however, the time reversed signal is generated right after the reading beam is allowed to pass and read the hologram, rendering a high peak standing

out of the background. The signal decays quickly because the reading beam at the same time erase the hologram stored in the crystal. The subtraction of signals with and without ultrasound modulation provides a signal as the red curve shown in Fig. 4(b), which is defined as the TRUE signal in the study. For comparison, in Fig. 4(b) we include altogether three TRUE signals obtained with different reading beam intensities under the otherwise identical conditions. As we can see a stronger reading beam yields a higher amplitude for the peak, but a shorter duration due to the faster erasure of the hologram, which is determined by the physical properties of the photorefractive material[10]. To focus deeper into the turbid medium, stronger reading beam thereby is usually preferred. However, for the safety of the optical components, we use 900 mW/cm^2 for the reading beam in our study.

3. RESULTS AND DISCUSSION

Since the strength of ultrasound modulation and the amount of ultrasonically-encoded photons are both closely related with the optical properties within the ultrasound focus[5, 11-14], so is the amplitude of TRUE signal. Therefore, the amplitude information of TRUE can be used to infer the feasibility and efficiency of optical focusing in tissue-mimicking phantom[8] and tissue[9].

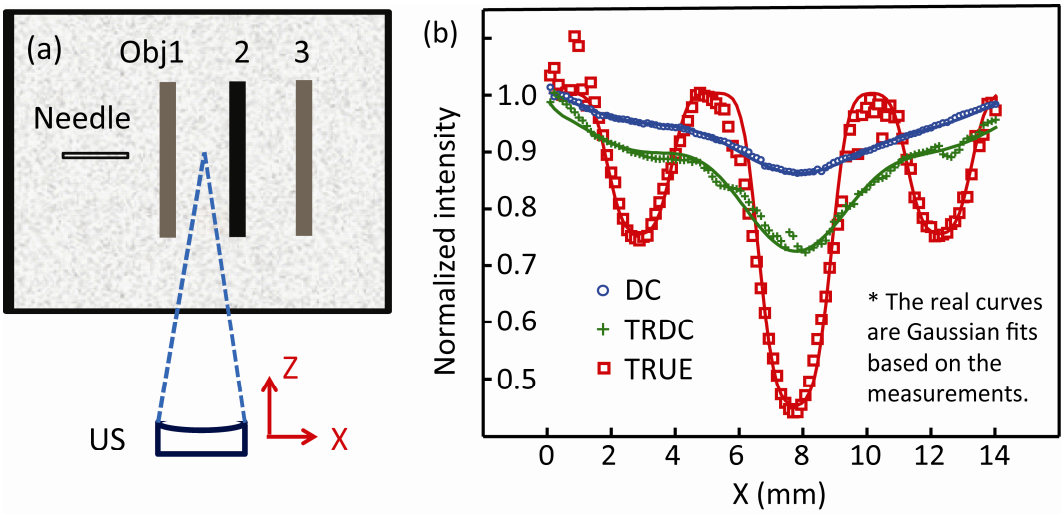

Fig. 5 (a) A phantom cross-section showing three embedded optical absorption objects aligned along the X direction. This cross- section was embedded 2 mm deep within the scattering medium as illustrated in Fig. 3. (b) The resulted TRUE signal amplitude (red squares) distribution as function of phantom X position. Profiles of direct signal beam intensity detected after the crystal (DC, blue circles), and time-reversed signal beam intensity without ultrasound modulation (TRDC, green crosses) are also included for comparison. The blue, green and red curves correspond to the Gaussian fit of the measured DC, TRDC and TRUE, respectively.

Fig. 5(a) shows the cross-section of a scattering phantom sample made of water (90% by volume), gelatin (10% by weight), and diluted Intralipid (2% by volume) such that it had an optical reduced scattering coefficient of 20 mm^{-1}. There are three ~ 1 mm wide inclusions that had higher optical absorption coefficients (0.4, 1, and 0.4 cm^{-1}, respectively, from left to right) than the background, with the optical contrast provided by Indian ink. The spacing between adjacent objects was about 4.5 to 4.8 mm. This cross-section was embedded 2 mm deep in a 6 mm thick scattering medium (as shown in Fig. 3). Before the experiment, the ultrasound field was aligned such that its focus intersected with the object centers in both Y and Z directions with the needle on the most left as the position indicator. During the experiment, the light and sound components

remained stationary, but the sample was scanned along the X direction at a step size of 0.127 mm. At each position, one TRUE signal was obtained and recorded as discussed in Fig. 4. The resulting TRUE signal amplitude profile is shown (red squares) in Fig. 5(b) as a function of phantom position in the X direction. As we can see, the objects give lower TRUE signal amplitude than the background due to their higher absorption coefficients, i.e. weaker modulation depth as well as less ultrasonically-encoded photons. Moreover, the higher the object's absorption is (Obj 2), the lower the TRUE signal amplitude. Also, we are able to tell the exact position, and dimension of each object, which are very close to their actual values. A Gaussian fit (red curve) was applied to the measured data[6], from which we conclude that the TRUE imaging has a spatial resolution of about 0.63 mm, approximating the ultrasound focal width (0.87 mm) divided by √2. It is so because the detected photons contributing to the TRUE response physically traverse the ultrasound focus twice. For comparison, we also include in Fig. 5(b) the distribution profiles of direct light intensity (DC, blue circles) detected after the crystal, and time-reversed signal intensity without ultrasound modulation (TRDC, green crosses). As we can see, both of them have broad resolutions, and lack the capability of resolving the three objects due to the light diffusion.

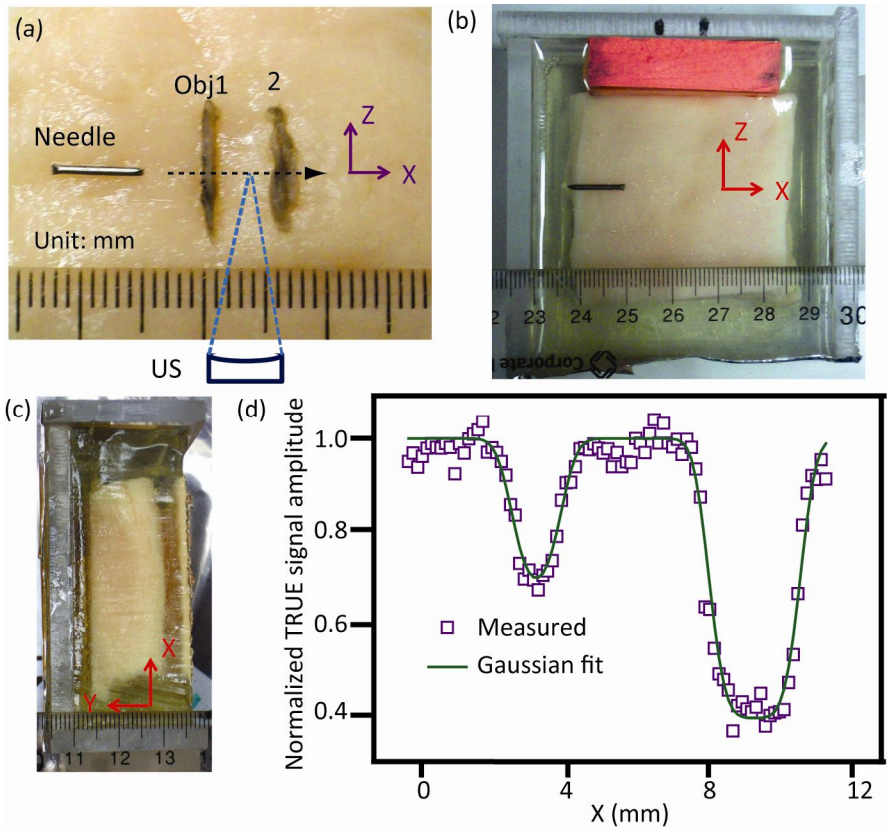

Fig. 6 (a) Cross-section of a chicken breast tissue containing two optical absorption inclusions and a needle for tissue sample alignment with respect to the ultrasound field and the incident light. This cross-section was embedded 2.5-3.0 mm deep in the Y direction in a tissue sample shown in the XZ plane (b) and XY plane (c). The tissue sample was surrounded by transparent gelatin gels within the sample holder, and the red rubber on the top was used to avoid strong acoustic reflection from the gelatin-air and gelatin-acrylic interfaces. (d) Resultant TRUE signal amplitude as a function of sample position in the X direction.

We also explored experimentally in *ex vivo* chicken breast to further confirm the feasibility and efficiency of TRUE optical focusing in real biological tissue. Similar to phantom sample preparation, in Fig. 6(a) we show a cross-section that was

embedded 2.5-3.0 mm deep along the Y direction. There were two absorption objects, separated about 6 mm in the X direction. Both of them were also chicken breast tissue pieces but dyed in Indian ink to have an optical absorption contrast with respect to the background. Fig. 6(b) and (c) show the outside geometry of the tissue sample in XZ and XY planes, respectively. To be noted that the top red rubber in Fig. 6(b) was used to minimize the acoustic reflections from the gelatin-air and gelatin-acrylic interfaces. In the same way as for the phantom sample, this tissue sample was scanned along the X direction, such that we obtained a TRUE signal amplitude distribution as a function of tissue sample position (Fig. 6d). From this profile, we are able to identify precisely the position and dimension of each object: Obj1 at X = 3.5 mm, about 0.75 mm wide, with a negative contrast (with respect to the background) of 32%; Obj2 at X = 9.6 mm, about 1.2 mm wide, with a negative contrast of 60%. The resultant spatial resolution told from the Gaussian fit is about 0.67 mm, very close to the value obtained in the phantom sample and the ultrasound focal width over square root of 2. This confirms that despite of the differences in optical and acoustic properties, TRUE optical focusing holds its validity in tissue as in phantom.

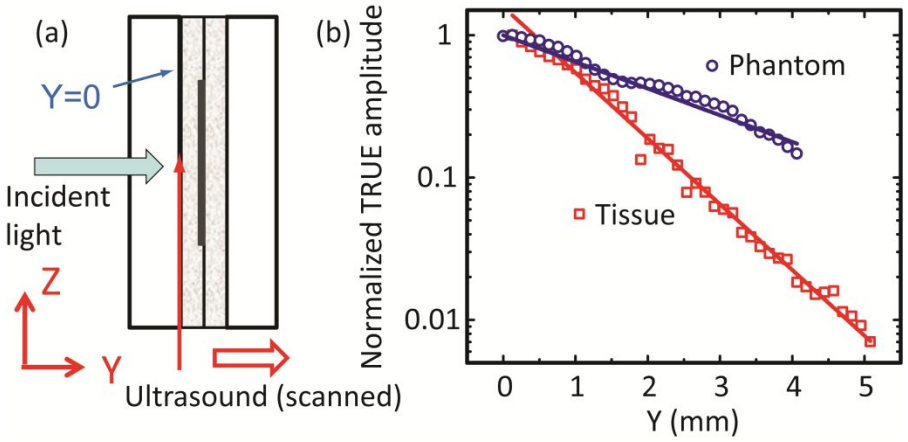

Fig. 7 (a) The ultrasound focus was scanned along the Y direction with respect to the samples. (b) TRUE signal amplitude as a function of ultrasound focus Y position in the phantom (purple circles) and the chicken breast sample (red squares), respectively.

That being said, we did observe differences regarding TRUE signal amplitude changes in phantom and in tissue when the ultrasound field was scanned along the Y direction as in Fig. 7(a). We noticed that in chicken breast TRUE signal amplitude decays much faster than in the phantom (Fig. 7b) with ultrasound focal depth in the scattering media. Considering that photons experience round trips for both hologram writing and reading stages in the reflection mode, the TRUE signal decay rate per mm is 0.21 and 0.51, respectively, in the phantom and the tissue. These are actually fairly close to the effective attenuation coefficients of that type of phantom and tissue: phantom, $\mu_s' = 2.0\,\text{mm}^{-1}$, $\mu_a = 0.008\ \text{mm}^{-1}$, $\mu_{eff} = \sqrt{3\times\mu_a(\mu_a+\mu_s')} = 0.22\ \text{mm}^{-1}$; breast tissue[15], $\mu_s' = 1.4\,\text{mm}^{-1}$, $\mu_a = 0.063\,\text{mm}^{-1}$, $\mu_{eff} = 0.53\,\text{mm}^{-1}$. Since μ_{eff} is the parameter describing the fluence decay rate of diffused light, this agreement, once again, confirms that TRUE focused diffused, but not ballistic, photons back into the ultrasound focus. It also suggests that the ultimate limit for TRUE is determined by the effective attenuation coefficient, not scattering coefficient, of the medium, which means under an ideal situation TRUE is able to focus light into tissue or tissue-like media several centimeters deep. We should bear in mind,

however, too high optical absorption will jeopardize the validity of the time reversal. With our current setup, the maximum optical penetration depth, defined by the product of medium diffusivity and focusing depth that is doubled, is 160 and 100, respectively, in the phantom and the chicken breast tissue. These are great improvements from previous maximum depth of 70 in phantom in transmission mode[7].

4. SUMMARY AND FUTURE WORK

In summary, we developed a reflection-mode TRUE optical focusing system using a large aperture fiber bundle for efficient and convenient diffused light collection and transmission. We experimentally validated optical focusing in both phantom and *ex vivo* tissue, with the focusing resolution determined by the ultrasound focal width divided by square root of 2. Current setup enables us to improve the maximum optical penetration depth up to 160 and 100 in phantom and tissue, respectively. It should be mentioned that TRUE is still in its infancy with a lot more be done. For example, in the near future, the system will be transited to 1064 nm optical wavelength to focus even deeper into tissue benefitting from less optical effective attenuation coefficient of tissue (from 0.53/mm at 532 nm to 0.16/mm at 1064 nm) and higher laser permissible level (from 0.2 W/cm^2 at 532 nm to 1.0 W/cm^2 at 1064 nm[16]). On the other hand, photorefractive crystal at 1064 nm (e.g. GaAs[17] and $Sn_2P_2S_6$:Te[18]) can response faster under strong illumination, making the system potential to overcome the *in vivo* speckle decorrelation (1-10 kHz) from physiological motions. Another important aspect is to improve the time reversal efficiency, possibly with a gain larger than 1, i.e., the reversed signal even stronger than the initial encoded light. We believe, not far from now, TRUE optical focusing will find broad biomedicine applications such as, but not limited to, fluorescent excitation, photoacoustic excitation, photodynamic therapy, and optical manipulation.

ACKNOWLEDGEMENT

This research is sponsored in part by the National Academies Keck Futures Initiative grant IS 13 and the National Institute of Health through grants R01 EB000712 and U54 CA136398. L.W. has a financial interest in Microphotoacoustics, Inc. and Endra, Inc., which, however, did not support this work.

REFERENCES

1. Wang, L. V. and Wu, H., Biomedical Optics: Principles and Imaging, John Wiley and Sons, Hoboken, New Jersey (2007).

2. Vellekoop, I. M. and Mosk, A. P., "Focusing coherent light through opaque strongly scattering media," Optics Letters 32, 2309-2311 (2007).

3. Vellekoop, I. M., van Putten, E. G., Lagendijk, A. and Mosk, A. P., "Demixing light paths inside disordered metamaterials," Optics Express 16, 67-80 (2008).

4. Yaqoob, Z., Psaltis, D., Feld, M. S. and Yang, C., "Optical phase conjugation for turbidity suppression in biological samples," Nature Photonics 2, 110-115 (2008).

5. Wang, L. V., "Mechanisms of ultrasound modulation of multiply scattered coherent light: An analytic model," Phys. Rev. Lett. 87, 043903 (2001).

6. Xu, X., Liu, H. and Wang, L. V., "Time-reversed ultrasonically encoded optical focusing into scattering media," Nature Photonics 5, 154-157 (2011).

7. Liu, H., Xu, X., Lai, P. and Wang, L. V., "Time-reversed ultrasonically encoded (TRUE) optical focusing into

tissue-mimicking media with optical thickness up to 70," Journal of Biomedical Optics 16, 086009 (2011).
8. Lai, P., Xu, X., Liu, H., Suzuki, Y. and Wang, L. V., "Reflection-mode time-reversed ultrasonically encoded (TRUE) optical focusing into turbid media," Journal of Biomedical Optics 16, 080505 (2011).
9. Lai, P., Xu, X., Liu, H. and Wang, L. V., "Time-reversed ultrasonically encoded (TRUE) optical focusing in biological tissue," Journal of Biomedical Optics (Accepted), (2012).
10. Solymar, L., Webb, D. J. and Jepsen, A. G., The Physics and Applications of Photorefractive Materials, Clarendon Press, Oxford (1996).
11. Sakadzic, S. and Wang, L. V., "Modulation of multiply scattered coherent light by ultrasound pulses: An analytical model," Phys. Rev. E 72, 033620 (2005).
12. Lai, P., Roy, R. A. and Murray, T. W., "Quantitative characterization of turbid medium using pressure contrast acousto-optic imaging," Optics Letters 34, 2850-2852 (2009).
13. Murray, T. W., Lai, P. and Roy, R. A., "Measuring tissue properties and monitoring therapeutic responses using acousto-optic imaging," Annals of Biomedical Engineering (2011, DOI:10.1007/s10439-011-0425-z).
14. Lai, P., McLaughlan, J. R., Draudt, A. B., Murray, T. W., Cleveland, R. O. and Roy, R. A., "Real time monitoring of high intensity focused ultrasound lesion formation using acousto-optic sensing," Ultrasound in Medicine and Biology 37, 239-252 (2011).
15. Kolzer, J., Mitic, G., Otto, J. and Zinth, W., "Measurement of the optical properties of breast tissue using time-resolved transillumination," SPIE 2326, 143-152 (1995).
16. American National Standards Institute, "American National Standard for the Safe Use of Laser in Health Care Facilities, ANSI Z1361.1," American National Standards Institute, New York (2000).
17. Gross, M., Lesaffre, M., Ramaz, F., Delaye, P., Roosen, G. and Boccara, A. C., "Detection of the tagged or untagged photons in acousto-optic imaging of thick scattering media by photorefractive adaptive holography," Eur. Phys. J. E 28, 173-182 (2009).
18. Farahi, S., Montemezzani, G., Grabar, A. A., Huignard, J. P. and Ramaz, F., "Photorefractive acousto-optic imaging in thick scattering media at 790 nm with a $Sn_2P_2S_6$:Te crystal," Optics Letters 35, 1798-1800 (2010).